Supporting Information for

Single Site Cobalt Substitution in 2D Molybdenum Carbide (MXene) Enhances Catalytic Activity in the Hydrogen Evolution Reaction

Denis A. Kuznetsov,[†] Zixuan Chen,[†] Priyank V. Kumar,[‡] Athanasia Tsoukalou,[†] Agnieszka Kierzkowska,[†] Paula M. Abdala,[†] Olga V. Safonova,[#] Alexey Fedorov[*,†] and Christoph R. Müller[*,†]

[†] ETH Zürich, Department of Mechanical and Process Engineering, CH 8092 Zürich, Switzerland

[‡] University of New South Wales, School of Chemical Engineering, Sydney, New South Wales 2052, Australia

[#] Paul Scherrer Institute, CH-5232 Villigen, Switzerland

Corresponding Authors:

*A.F.: fedoroal@ethz.ch

*C.R.M.: muelchri@ethz.ch

GENERAL EXPERIMENTAL

Synthesis. *β-Mo_2C:Co*. Ammonium heptamolybdate tetrahydrate $(NH_4)_6Mo_7O_{24}\cdot 4H_2O$ (5.0 g, 99 %, Alfa Aesar) and cobalt nitrate hexahydrate $Co(NO_3)_2\cdot 6H_2O$ (1.237 g, 99 %, Acros Organics), molar ratio 1:0.15, were dissolved in 150 ml of deionized water to produce a clear red solution. Subsequently, the solvent was evaporated by heating at 100 °C in an oven. The dry residue was ground in a mortar to yield a fine pink powder which was carburized in a quartz reactor (750 °C, 10 °C min^{-1}, H_2/CH_4 (80/20 vol. %), 50 ml min^{-1}, 3 h) giving β-Mo_2C:Co as a black solid.

Mo_2Ga_2C:Co. Preparation of Mo_2Ga_2C was conducted according to the reported literature procedure.[1] As-synthesized β-Mo_2C:Co (2 g) was homogeneously mixed with metallic Ga (99.99 %, Acros Organics), molar ratio β-Mo_2C:Co : Ga = 1 : 12 (8.20 g Ga), in a mortar. This amount of Ga is required to ensure homogenous mixing and formation of a paste-like material. The obtained paste was transferred to a quartz tube, evacuated to *ca.* 10^{-5} mbar, flame-sealed under dynamic vacuum and annealed for 48 h at 850 °C (10 °C min^{-1}). The as-prepared material was first stirred in aqueous HF (50 mL, ≥ 48%, Sigma Aldrich) for 72 h at room temperature to remove excess unreacted metallic Ga and metallic Co remaining from the synthesis of β-Mo_2C:Co. The obtained solid residue was washed with DI water until a pH of *ca.* 6 was reached. Drying in air at 80 °C for 12 h produced the desired Mo_2Ga_2C:Co phase.

Mo_2CT_x:Co. The MXene phase, Mo_2CT_x:Co, was synthesized by etching Ga from Mo_2Ga_2C:Co following a recently reported literature protocol.[1] Mo_2Ga_2C:Co (1 g) and 50 mL of ≥ 48% HF were stirred at 140 °C for 7 days in a sealed Teflon lined stainless steel Parr autoclave placed in a sand bath. Important: experiments with concentrated HF at high temperatures as used in this work required extra care and were conducted in an HF-dedicated fume hood at the specialized Toxlab of ETH Zürich. The resulting suspension was centrifuged at 5000 rpm for 3 min to separate the solid product, which was repeatedly washed with DI water until a pH of washings reached ca. 6. The solid obtained was dried in air at 80 °C for 12 h.

Characterization. X-ray powder diffraction (XRD) data were collected on a PANalytical Empyrean X-ray diffractometer equipped with a Bragg–Brentano HD mirror and operated at 45 kV and 40 mA using CuKα radiation (λ = 1.5418 Å). The Le Bail fitting of the XRD patterns[2] was preformed using Fullprof software.[3] Scanning electron microscopy (SEM) measurements were performed on a FEI Magellan 400 FEG microscope. Prior to imaging, the samples were sputter coated with an *ca.* 5 nm thick layer of PtPd (CCU-010 Metal Sputter Coater Safematic). TEM imaging was performed using a FEI Talos F200X microscope equipped with a high-brightness field-emission gun, a high-angle annular dark field (HAADF) detector, and a large collection-angle EDX detector. The operation voltage of the instrument was set to 200 kV in scanning transmission electron microscopy (STEM) mode. To prepare the sample for TEM measurements, dried powder of Mo_2CT_x:Co (100 mg) was dispersed in a 10 % aqueous solution of tetrabutylammonium hydroxide (TBAOH) (Sigma Aldrich) (5 ml) and stirred overnight.[4] The solid residue was separated from the solution by centrifugation and washed 3 times with water (20 ml) and 3 times with ethanol (20 ml) to remove excess TBAOH. The powder was then sonicated with 5 ml of ethanol for 1 h in an ice-cooled ultrasonic bath. The dark purple colloidal solution was separated from the solid by centrifugation at 3500 rpm for 30 min. This solution was drop cast onto Cu grids coated with carbon for TEM measurements. X-ray photoelectron spectroscopy (XPS) measurements were conducted on a Sigma 2 instrument (Thermo Fisher Scientific) equipped with an UHV chamber (non-monochromatic 200 W Al Kα source, a hemispherical analyzer, and a seven

channel electron multiplier). The analyzer-to-source angle was 50°, while the emission angle was 0°. A pass energy of 50 eV and 25 eV was set for the survey and the narrow scans, respectively. The C 1 s peak of adventitious carbon was set at 284.8 eV to compensate for any charge induced shifts. XPS data were analyzed with the CasaXPS software. Elemental Analysis measurements were performed by the Mikroanalytisches Labor Pascher, Germany.

X-ray absorption spectroscopy (XAS) measurements (Co K-edge) were performed at the SuperXAS beamline of the Swiss Light Source (SLS) (PSI, Villigen, Switzerland). The incident photon beam provided by a 2.9 T superbend magnet was selected by a Si (111) channel-cut monochromator. The rejection of higher harmonics and focusing were achieved by a Si-coated collimating mirror at 2.5 mrad and a rhodium-coated torroidal mirror at 2.5 mrad. Co K-edge XAS data for the reference samples (Co, CoO, Co_3O_4) were collected in transmission mode from pellets of the corresponding materials composed of the optimized amount of sample mixed with cellulose. For Co-doped carbides, the Co K-edge XAS spectra were collected on pure materials in fluorescence mode using a five-element silicon drift detector (SGX). XAS data processing was performed using the Athena software and EXAFS fitting was performed with the Artemis software (Demeter 0.9.25 software package). For EXAFS data analysis, the spectra were converted to the photoelectron wave vector k ($Å^{-1}$). The resulting $\chi(k)$ functions were k^2 weighted and Fourier transformed over the 2.7−10 $Å^{-1}$ range.

The samples of Mo_2CT_x:Co after HER experiments for XAS, XPS and SEM investigation were prepared by attaching a pellet of Mo_2CT_x:Co (9 mm diameter, *ca.* 70 mg) to a graphene paper (120 µm thickness, Sigma Aldrich) with a conductive carbon glue (Ted Pella). The electrode was held at −0.25 V vs. RHE for 15 min. Intensive H_2 bubbles formation was observed during experiment. The pellet was carefully rinsed with DI water to remove H_2SO_4 and air-dried.

Electrochemical measurements. HER measurements were performed in a conventional three-electrode cell setup, using a rotating disk-electrode with deposited catalyst ink as a working electrode, Hg/Hg_2SO_4 reference electrodes and a graphite rod counter electrode, in H_2-saturated 1 N H_2SO_4. The catalyst ink was prepared by adding 10 mg MXene powder to 0.99 ml absolute ethanol followed by the addition of 0.01 ml of *ca.* 20 % Nafion solution. This slurry was sonicated for 1 h, and 20 µl of the ink was drop cast on the polished (0.03 µm) glassy carbon electrode (0.196 cm^{-2} surface area) resulting in a MXene loading of 1 mg cm_{geo}^{-2}. For the preparation of the electrodes with a MXene loading of 0.1 mg cm_{geo}^{-2}, 10 mg MXene powder, 4.95 ml of absolute ethanol and 0.05 ml of ca. 20 % Nafion solution were mixed and 10 µl of the ink was drop cast on the glassy carbon electrode. The Hg/Hg_2SO_4 reference electrode was calibrated versus RHE in the same electrolyte saturated with H_2, after HER measurements, by either measuring the voltage, E_{offset}, corresponding to zero current (from CV scan at 1 mV s^{-1}) from hydrogen oxidation/evolution on a platinum electrode or measuring the open circuit voltage. This voltage value was defined as 0 V vs. RHE (which corresponds to −0.704 V vs. Hg/Hg_2SO_4 in 1 N H_2SO_4). Note that measurements of HER currents should be performed under the same conditions (pH, P_{H2}) for which the reference potential was established, i.e. H_2 saturation. Indeed, HER measurements under Ar saturation may result in apparent decrease of the overpotential, however this artifact can merely be due to the dependence of $E_{H2/H+}$ on H_2 partial pressure, according to Nernst equation (eq. 1), which will not be accounted for by converting $E_{measured}$ to E_{RHE} via a simple addition of E_{offset} term, determined during calibration as a voltage corresponding to zero current from hydrogen oxidation/evolution on a platinum electrode[5] (see above):

$$E_{H2/H+} = E_{H2/H+}^{0} + RT/nF \cdot \ln(a_{H+}/P_{H2}) \quad \text{(eq. 1)}$$

where $E_{H2/H+}{}^0$ – H_2/H^+ is equilibrium potential, 0 V vs. NHE (pH 0, 1 atm H_2 pressure), a_{H+} - H^+ activity in solution, P_{H2} –partial pressure of H_2 in solution

Correction for ohmic losses (iR correction) was done by subtracting the ohmic voltage drop from the measured potential, using the resistance value determined by impedance measurements. Steady-state galvanostatic measurements of the HER activity were performed by applying incrementally increased negative currents, and the potentials corresponding to the plateau of the E-t curves were used for plotting Tafel dependencies.

The electrochemically active surface area (ECSA) of the electrodes was estimated via the measurements of the electrode area-normalized double layer capacitance (C_{dl}) by recording the scan rate-dependence of the non-Faradaic capacitive current that is associated with double-layer charging, as demonstrated for a representative electrode in Figure S11. The average C_{dl} values (5.4 mF cm^{-2} for Mo_2CT_x:Co and 1.8 mF cm^{-2} for Mo_2CT_x) were converted to ECSA using the equation ECSA = C_{dl}*S/C_s, where S is the geometric surface area of the electrode, C_s is the specific capacity of a flat metal surface (0.04 mF cm^{-2})[6] resulting in ECSA values of 26.7 cm^2 for Mo_2CT_x:Co [135 $cm_{ECSA}{}^2$ $cm_{geo}{}^{-2}$, or 135 $m_{ECSA}{}^2$ g^{-1}] and 8.9 cm^2 for Mo_2CT_x [45 $cm_{ECSA}{}^2$ $cm_{geo}{}^{-2}$, or 45 $m_{ECSA}{}^2$ g^{-1}]. These values were used to normalize the currents.

DFT calculations. All structural relaxation calculations were performed using a plane-wave basis set as implemented in the VASP package until the residual forces acting on atoms were less than 0.03 eV/Å.[7,8] We employed the Projector Augmented Wave (PAW) method to describe the core electrons[9] and the Perdew Burke Ernzerhof exchange-correlation (XC) functional.[10] The kinetic energy cutoff for the wave function and charge density was set to 450 eV, and a gamma-point k-grid was used for the 4 × 4 × 1 unit cell calculations. A vacuum region greater than 12 Å was used in the direction normal to the sheets to avoid interaction between neighboring images.

The differential hydrogen adsorption energy, ΔE_{H}, was calculated as:

$$\Delta E_{\mathrm{H}} = E_{\mathrm{system}+n\mathrm{H}} - E_{\mathrm{system}+(n-1)\mathrm{H}} - {}^1\!/_2\, E_{\mathrm{H_2}} \qquad \text{(eq. 2)}$$

where, $E_{\mathrm{system}+n\mathrm{H}}$ is the total energy of the Mo_2CO_2 or the Co-substituted Mo_2CO_2 system with n adsorbed hydrogen atoms, $E_{\mathrm{system}+(n-1)\mathrm{H}}$ is the total energy of the same system with (n-1) adsorbed hydrogen atoms and $E_{\mathrm{H_2}}$ is the energy of a hydrogen molecule in the gas phase. The free energy of hydrogen adsorption was then calculated as $\Delta G_{\mathrm{H}} = \Delta E_{\mathrm{H}} + 0.37$ eV, where ΔE_{H} is the differential hydrogen adsorption energy as computed above, and the value of 0.37 eV, which is taken from ref.[11] includes changes in the zero-point energy and the entropy between the adsorbed state and the gas phase of hydrogen.

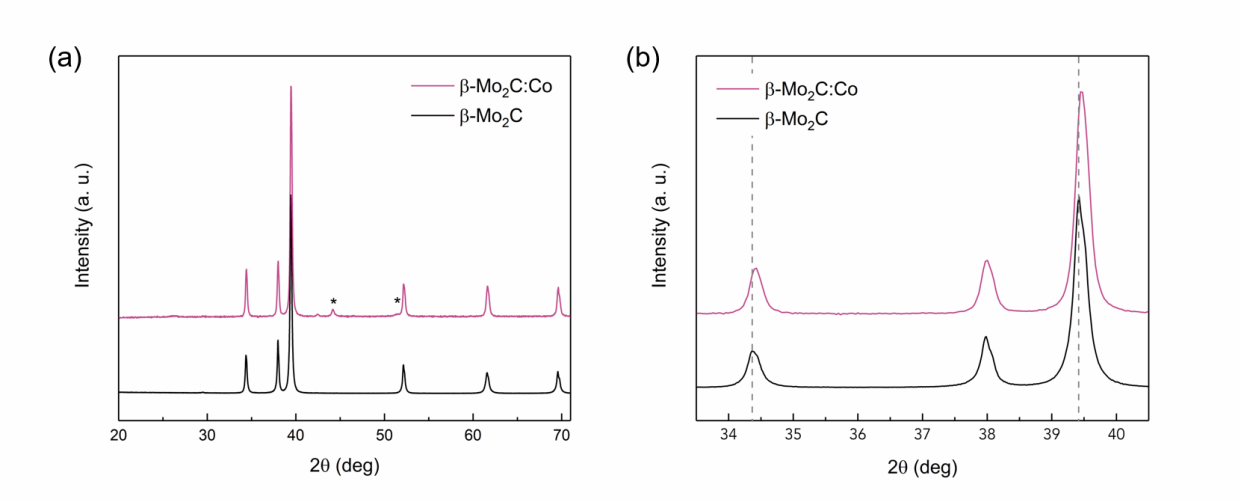

Figure S1. (a) XRD patterns of as-synthesized β-Mo_2C:Co and commercial β-Mo_2C (peaks due to metallic Co impurity are labelled by asterisks), and (b) magnified 34-40 ° region highlighting (100) and (101) peak shifts towards higher diffraction angles upon Co doping.

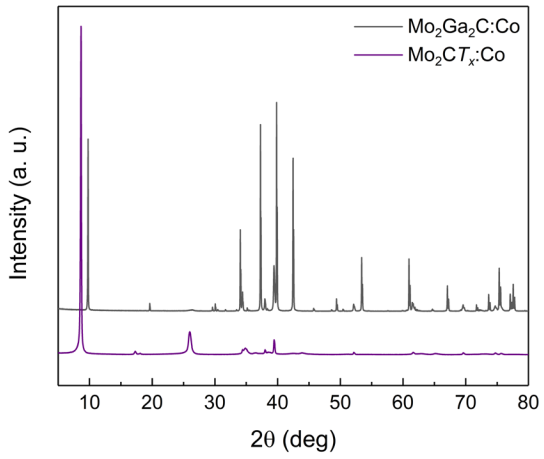

Figure S2. XRD patterns for Mo_2Ga_2C:Co and Mo_2CT_x:Co.

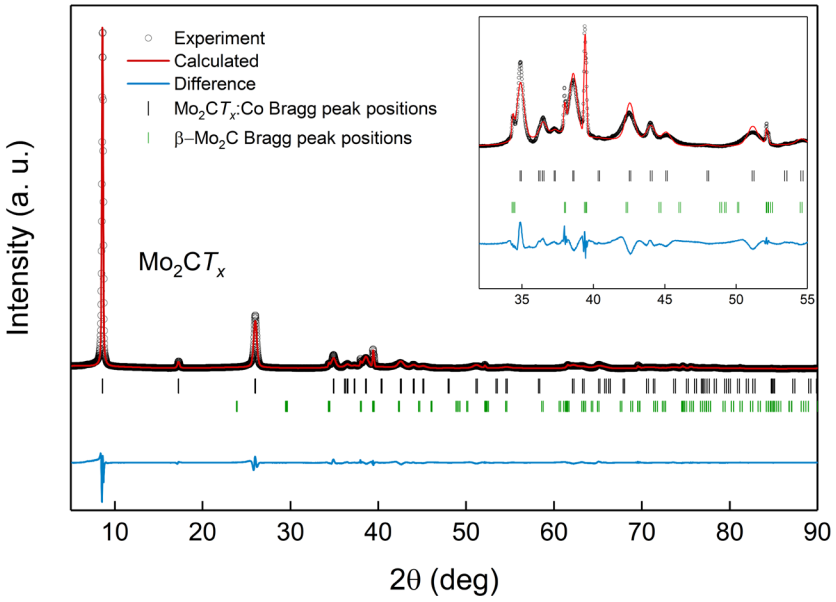

Figure S3. Le Bail fit for Mo_2CT_x material revealing that all reflections could be assigned to Mo_2CT_x and β-Mo_2C phases.

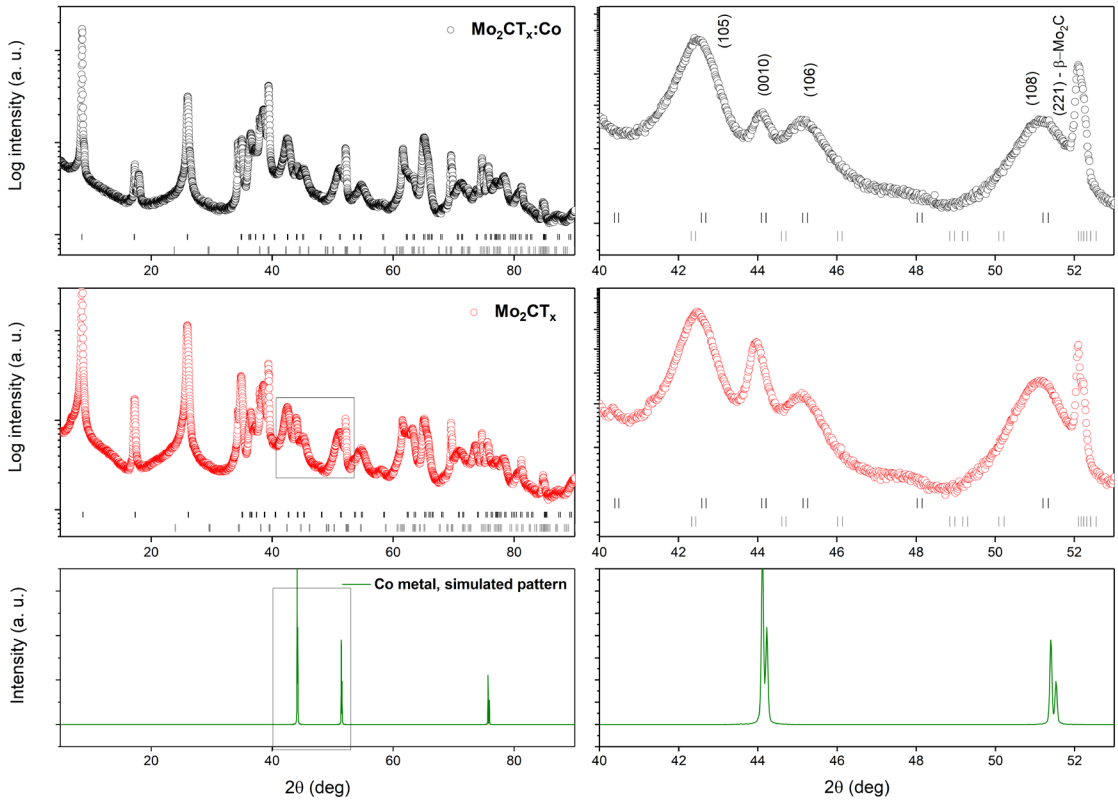

Figure S4. Experimental XRD patterns for Mo_2CT_x:Co, Mo_2CT_x (log intensity coordinates) revealing an identical set of peaks for both MXene materials. All peaks are indexed as *P6₃/mmc* space group, Miller indices are shown for the Mo_2CT_x:Co phase. Only the peak at ~52° belongs to β-Mo_2C. Simulated XRD pattern of metallic Co is shown for comparison, demonstrating that no peaks attributed to metallic Co can be found on the XRD pattern of Mo_2CT_x:Co.

Table S1. Extracted intensities for Mo_2CT_x:Co from Le Bail fitting of the experimental data.

No.	h	k	l	Multiplicity	2θ (deg)	I_{calc}	I_{obs}	d-hkl
1	0	0	2	2	8.591	106176.1	106176.4	10.28371
2	0	0	4	2	17.232	3210.2	3210.2	5.141857
3	0	0	6	2	25.972	35779	35779.1	3.427904
4	0	0	8	2	34.869	9766.2	9766.1	2.570928
5	1	0	0	6	36.176	0	0	2.480994
6	1	0	1	12	36.448	2764.1	2763.9	2.463138
7	1	0	2	12	37.252	1027	1027.1	2.411799
8	1	0	3	12	38.56	11621.7	11621.5	2.332933
9	1	0	4	12	40.331	104.1	104.1	2.234481
10	1	0	5	12	42.517	7669.8	7669.7	2.124489
11	0	0	10	2	43.99	3479.7	3479.8	2.056742
12	1	0	6	12	45.072	2499.3	2499.2	2.009818
13	1	0	7	12	47.953	353	353	1.895603
14	1	0	8	12	51.122	4762.8	4762.9	1.785275
15	0	0	12	2	53.414	127.6	127.6	1.713952
16	1	0	9	12	54.551	1802.2	1802.2	1.68087
17	1	0	10	12	58.219	278.6	278.5	1.583403
18	1	0	11	12	62.111	6203.9	6204.4	1.493203
19	0	0	14	2	63.246	3050.8	3050.8	1.469102
20	1	1	0	6	65.063	4826.5	4824.3	1.432403
21	1	1	2	12	65.77	1545.4	1547.8	1.418706
22	1	0	12	12	66.219	0.2	0.2	1.410171
23	1	1	4	12	67.868	101.5	101.5	1.379861
24	1	0	13	12	70.543	1988.2	1988.6	1.333962
25	1	1	6	12	71.299	1205.9	1205.9	1.321655
26	0	0	16	2	73.63	2288.4	2288.5	1.285464
27	1	0	14	12	75.086	424.8	425	1.264105
28	1	1	8	12	75.991	1088.9	1090.4	1.251295
29	2	0	0	6	76.772	265.4	264.3	1.240497
30	2	0	1	12	76.937	320.2	319.7	1.238247
31	2	0	2	12	77.432	448.3	449.1	1.231569
32	2	0	3	12	78.254	1360.6	1360.6	1.220676
33	2	0	4	12	79.401	0	0	1.205899

34	1	0	15	12	79.863	0	0	1.20008
35	2	0	5	12	80.869	798.2	798.3	1.187667
36	1	1	10	12	81.889	0	0	1.175431
37	2	0	6	12	82.656	0	0	1.166467
38	2	0	7	12	84.758	22.7	22.4	1.142818
39	0	0	18	2	84.775	26.8	26.6	1.142635
40	1	0	16	12	84.892	84.8	85.7	1.14136
41	2	0	8	12	87.175	678.9	678.9	1.117241
42	1	1	12	12	88.989	236	236.1	1.099105
43	2	0	9	12	89.909	687.2	686.7	1.090231

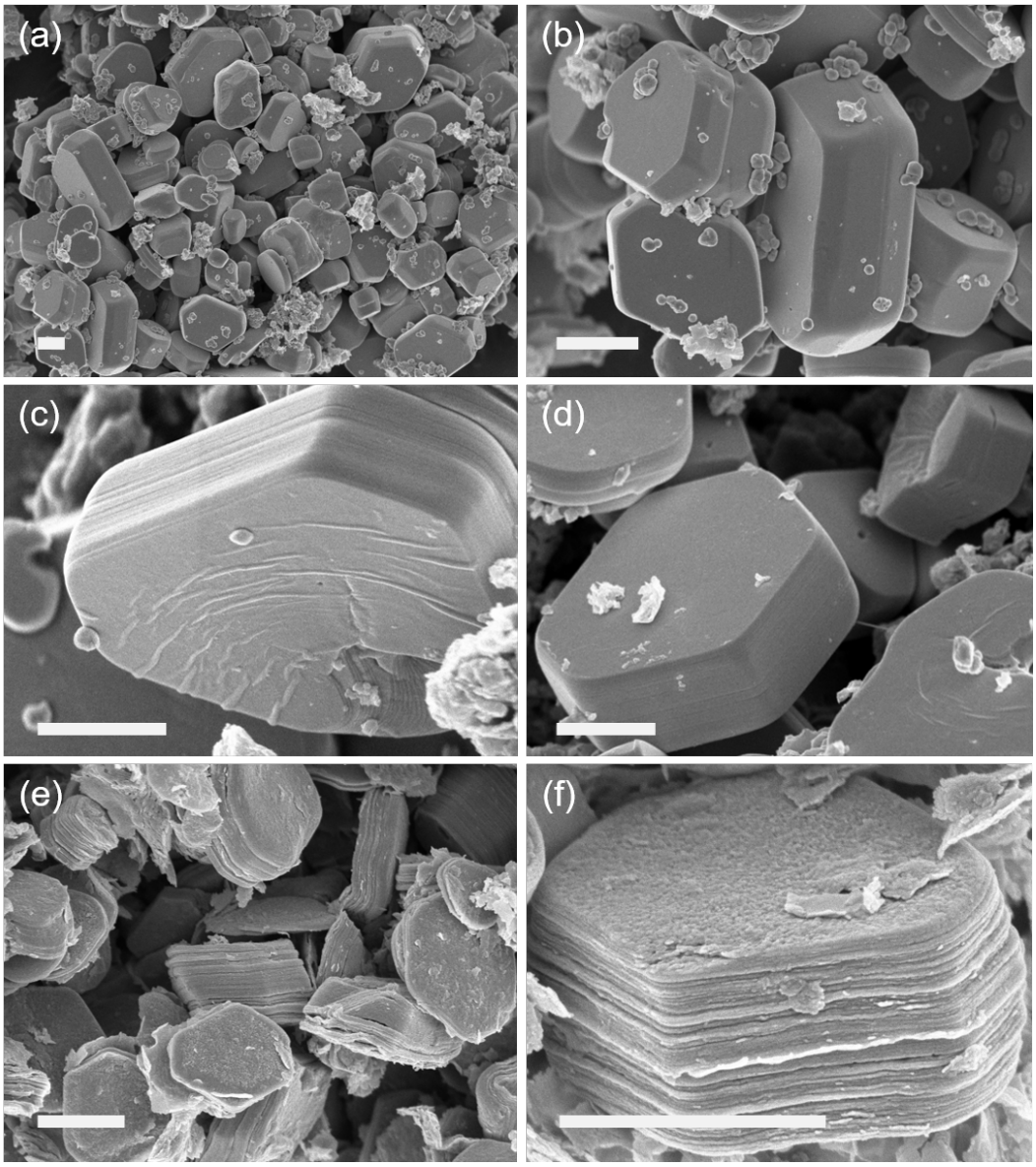

Figure S5. SEM images of Mo_2Ga_2C:Co (a, b) and Mo_2CT_x:Co before (c, d) and after (e, f) intercalation of TBAOH and sonication. Scale bar is 1 μm.

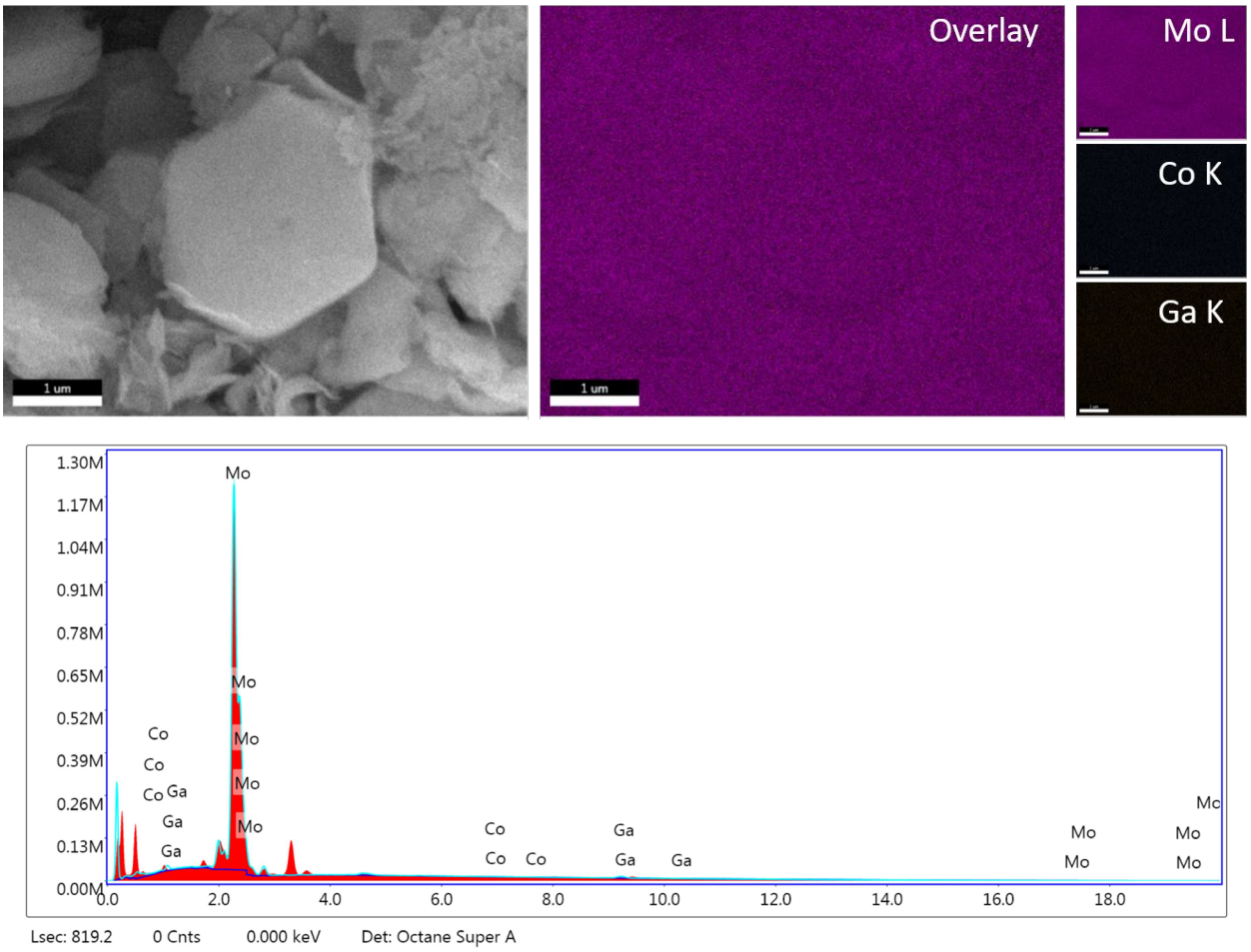

Element	Weight %	Atomic %	Net Int.	Error %	Kratio	Z	A	F
MoL	97.80	96.97	27077.30	1.16	0.9673	0.9990	0.9901	1.0000
CoK	0.09	0.15	16.90	30.28	0.0010	1.1080	0.9315	1.0517
GaK	2.11	2.88	221.60	4.25	0.0246	1.0646	0.9752	1.1228

Figure S6. Results of the EDX mapping for the representative area of Mo_2CT_x:Co sample. Carbon, oxygen, fluorine are not included, only metallic elements are shown. Data demonstrate that Co content is too low to be reliably quantified by EDX.

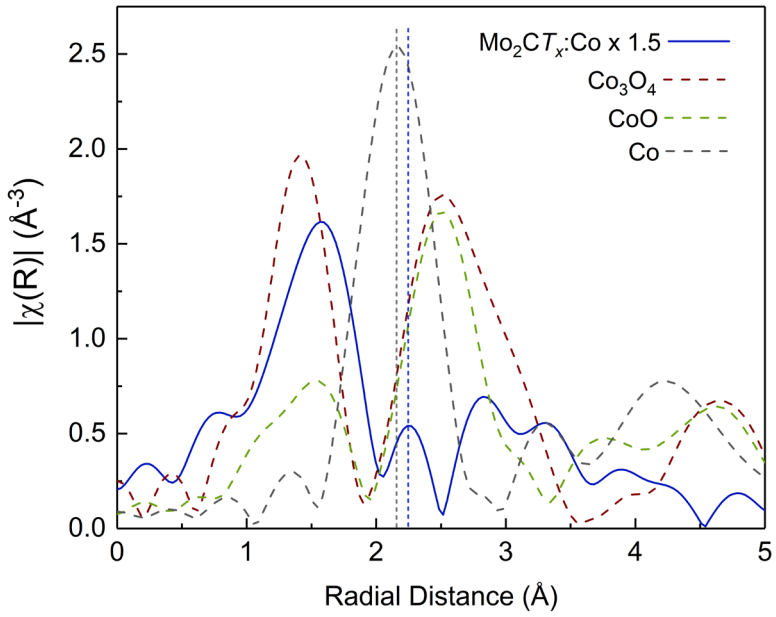

Figure S7. Comparison of the phase-uncorrected Fourier-transform of the Co K-edge EXAFS spectra of Mo_2CT_x:Co and Co, CoO, Co_3O_4 reference materials.

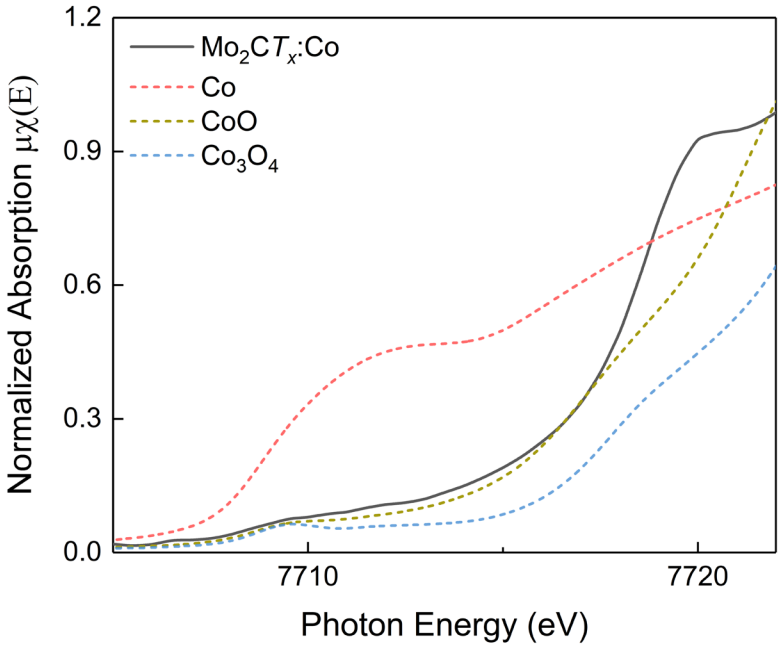

Figure S8. Comparison of the pre-edge regions of the normalized Co K-edge XANES spectra for Mo_2CT_x:Co and Co, CoO, Co_3O_4 reference materials.

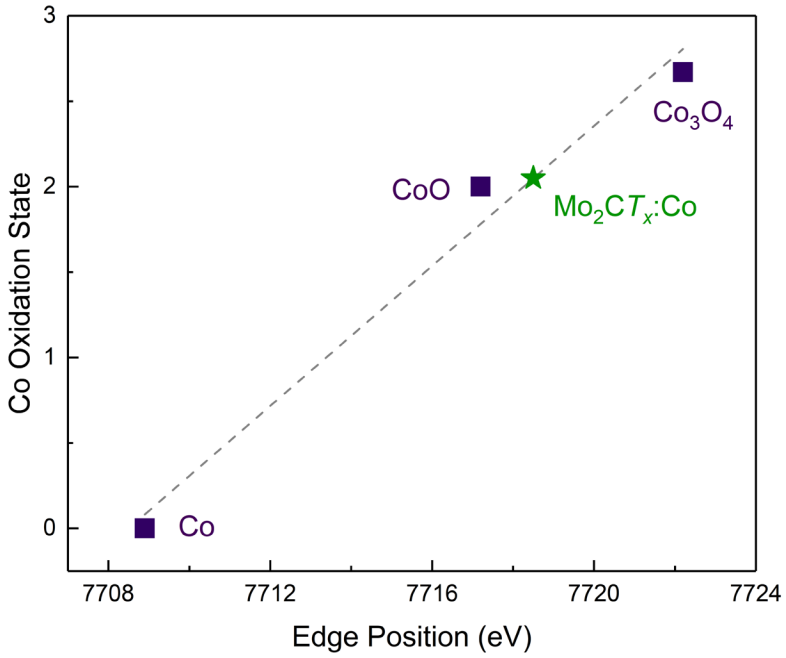

Figure S9. Estimation of the cobalt oxidation state in Mo_2CT_x:Co from the edge position in the XANES spectra of references Co, CoO, Co_3O_4.

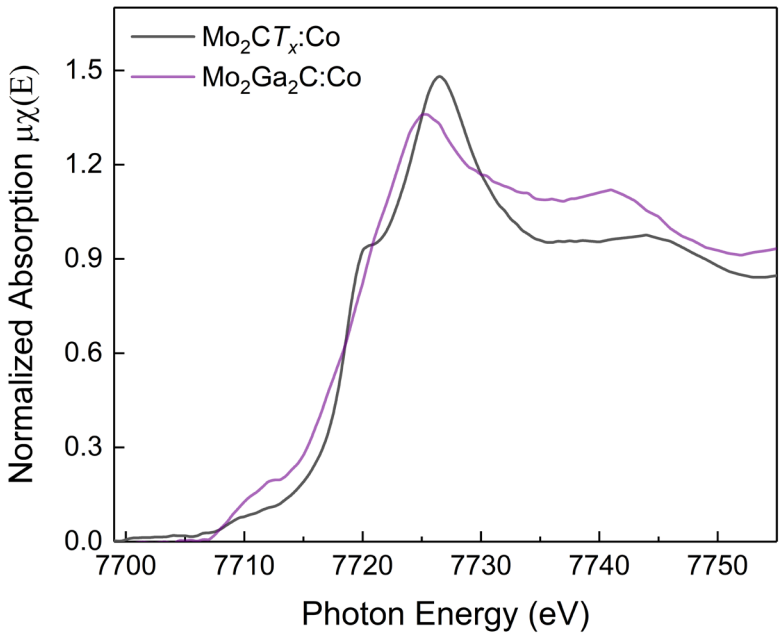

Figure S10. Comparison of the Co K-edge XANES spectra of Mo_2CT_x:Co and Mo_2Ga_2C:Co materials.

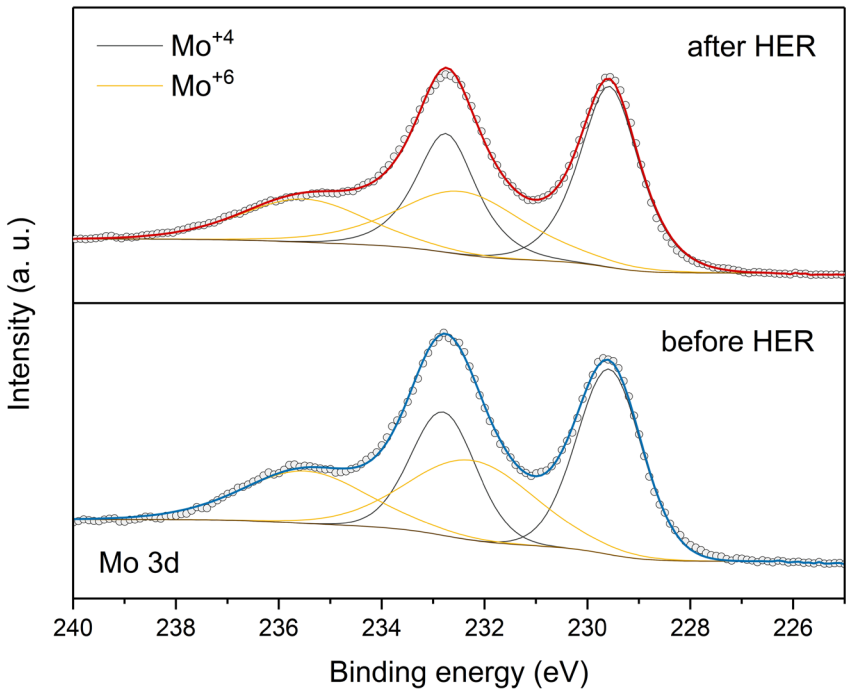

Figure S11. Core-level Mo 3d spectra of Mo_2CT_x:Co before and after HER measurements.

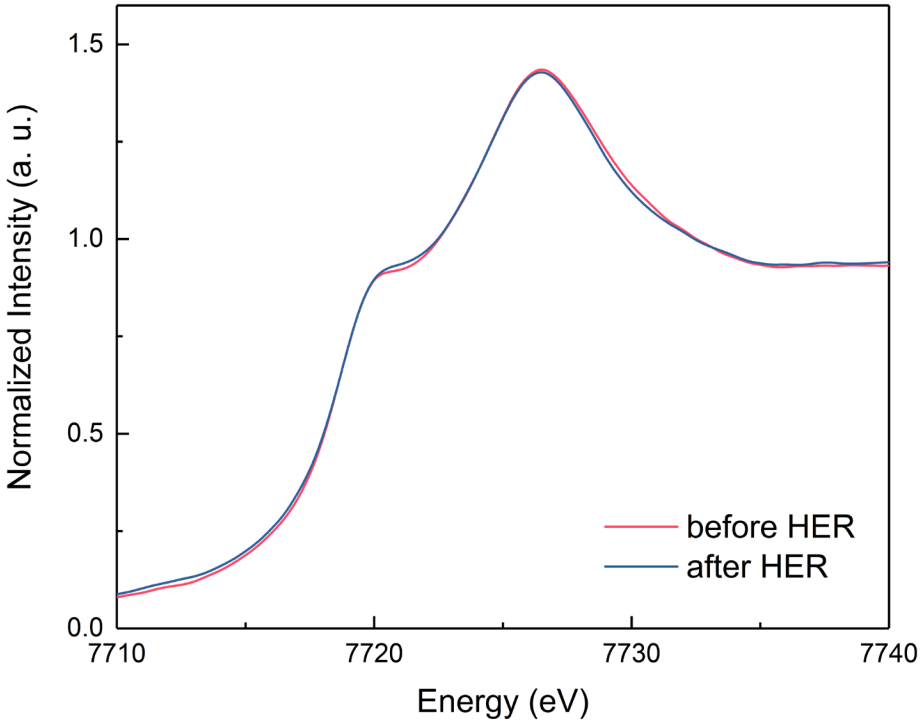

Figure S12. Comparison of the normalized Co K-edge XANES spectra of Mo_2CT_x:Co before and after HER measurements.

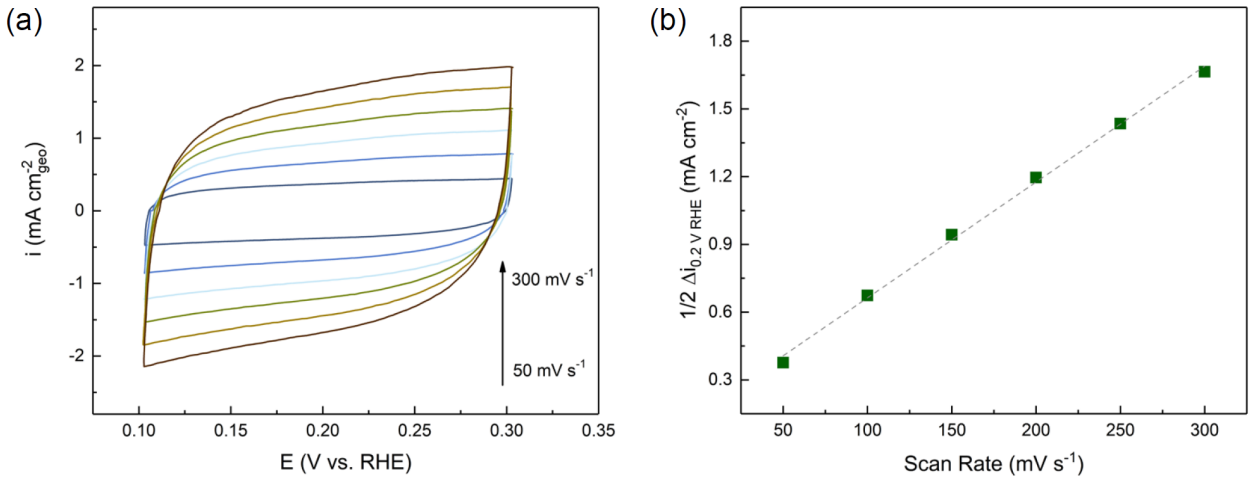

Figure S13. (a) CV scans recorded in the non-Faradaic region for a representative Mo_2CT_x:Co-based electrode using scan rates of 50, 100, 150, 200, 250, 300 mV s^{-1} in 1N H_2SO_4 electrolyte. (b) Scan rate dependence of the current density of a Mo_2CT_x:Co-based electrode from panel (a) used to determine the area normalized double layer capacity (C_{dl}) corresponding to the slope of the linear fit shown with a dashed line. The calculated C_{dl} value for a given electrode is 5.1 mF cm^{-2}, average capacity value of Mo_2CT_x:Co-based electrodes used to generate Tafel plots presented in the main text is 5.4 mF cm^{-2}.

To estimate the intrinsic activity of the catalysts, we calculated the average turnover frequency (TOF), using equation 3:

$$\mathrm{TOF} = \frac{\mathrm{n\ (H_2)}}{\mathrm{N(O)}} \qquad \text{(eq. 3)}$$

where TOF – turnover frequency (H_2 s^{-1})

n (H_2) – amount of H_2 produced per unit of electrode area per second (mol H_2 cm^{-2} s^{-1})

N (O) – number of O sites (active sites) per unit of electrode area (mol cm^{-2})

Here, we assume that all accessible O sites are catalytically active, that gives a conservative estimation of the number active sites (lower boundary).

Amount of H_2 produced per unit of electrode area per second (n(H_2), mol H_2 cm^{-2} s^{-1}):

$$\mathrm{n(H_2)} = \frac{|j|}{2F} \qquad \text{(eq. 4)}$$

where j is the current density (A cm^{-2}) and F is the Faraday constant (96485 C mol^{-1}). Coefficient 1/2 accounts for 2 electrons required to reduce protons to form a H_2 molecule.

n (H_2) = j [A cm^{-2}] · $5.182 \cdot 10^{-6}$ mol C^{-1} = j [mA cm^{-2}] · $5.182 \cdot 10^{-9}$ mol C^{-1}

Number of active sites (O atoms) per electrode surface area (mol cm^{-2})

$$\mathrm{N(O)} = \frac{S_{ECSA}}{S(O) \cdot S_{el}} \cdot \frac{1}{N_A} \qquad \text{(eq. 5)}$$

where S_{ECSA} is the experimentally-determined, electrochemically active surface area (cm^2)

S(O) is unit area containing one oxygen atom (cm^2)

S_{el} is the apparent electrode surface area (0.196 cm^2)

N_A is the Avogadro constant ($6.022 \cdot 10^{23}$ mol^{-1})

To estimate the number of oxygen atoms (active sites) per unit of electrode area, we have calculated the area of Mo_2CO_2 containing one oxygen atom (S(O), cm^2), using geometric parameters from the DFT optimized model:

$$S(O) = r^2 \cdot \sin \alpha \qquad \text{(eq. 6)}$$

where r is the O-O distance (2.89 Å = $2.89 \cdot 10^{-8}$ cm)

α – ∠O-O-O (60º, see Fig. S9)

S(O) = 7.23 $Å^2$ = $7.23 \cdot 10^{-16}$ cm^2

N(O) = 26.7 cm^2 / ($7.23 \cdot 10^{-16}$ cm^2 * 0.196 cm^2 * $6.022 \cdot 10^{23}$ mol^{-1}) = $3.13 \cdot 10^{-7}$ mol cm^{-2}

TOF = j [mA cm^{-2}] $\cdot 5.182 \cdot 10^{-9}$ mol C^{-1} / $3.13 \cdot 10^{-7}$ mol cm^{-2} = j * $1.656 \cdot 10^{-2}$ s^{-1}

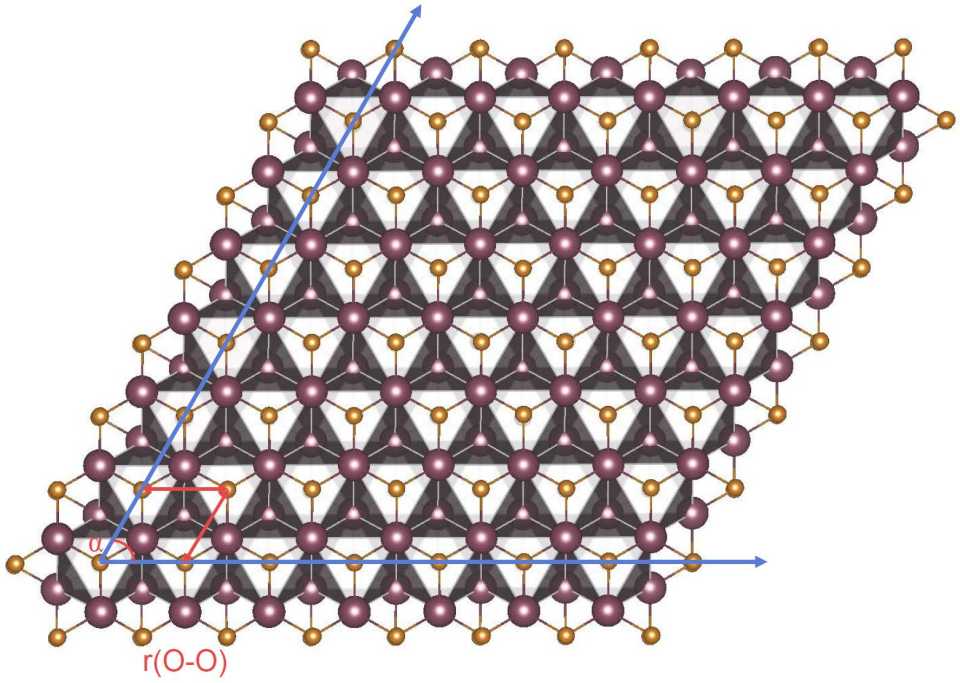

Figure S14. Model of Mo_2CT_x structure demonstrating the estimation of the average area containing one oxygen atom. Geometry parameters were taken from DFT calculations and are: r(O–O) = 2.89 Å, α = 60º.

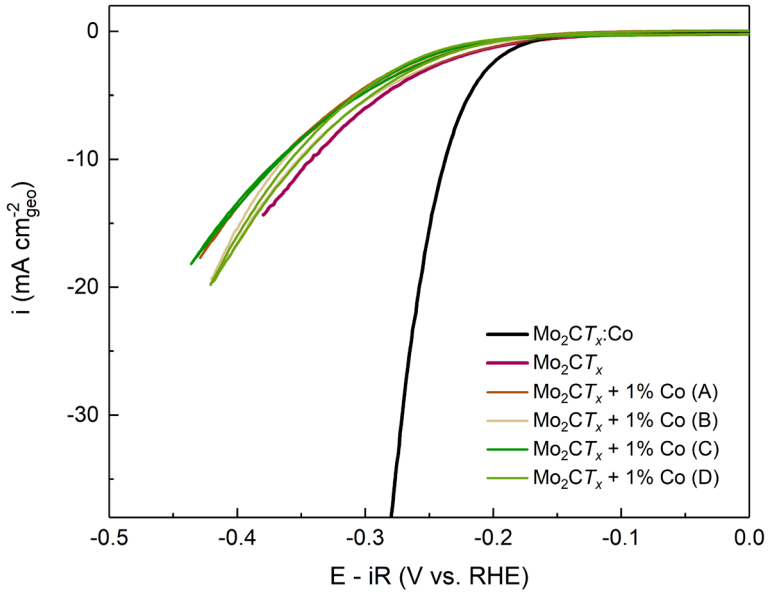

Figure S15. Polarization curves recorded for Mo_2CT_x:Co, Mo_2CT_x and Mo_2CT_x mixed with 1 wt. % Co powder (325 mesh) with a scan rate of 10 mV s^{-1}. All powders were deposited on glassy carbon electrodes with catalyst loading 0.1 mg cm^{-2} and measured in 1 N H_2SO_4. Data for Mo_2CT_x:Co and Mo_2CT_x are the same as presented in the main text. For (Mo_2CT_x + 1% Co) sample, four independent measurements are shown, highlighting no observable effect of the presence of metallic cobalt on HER activity.

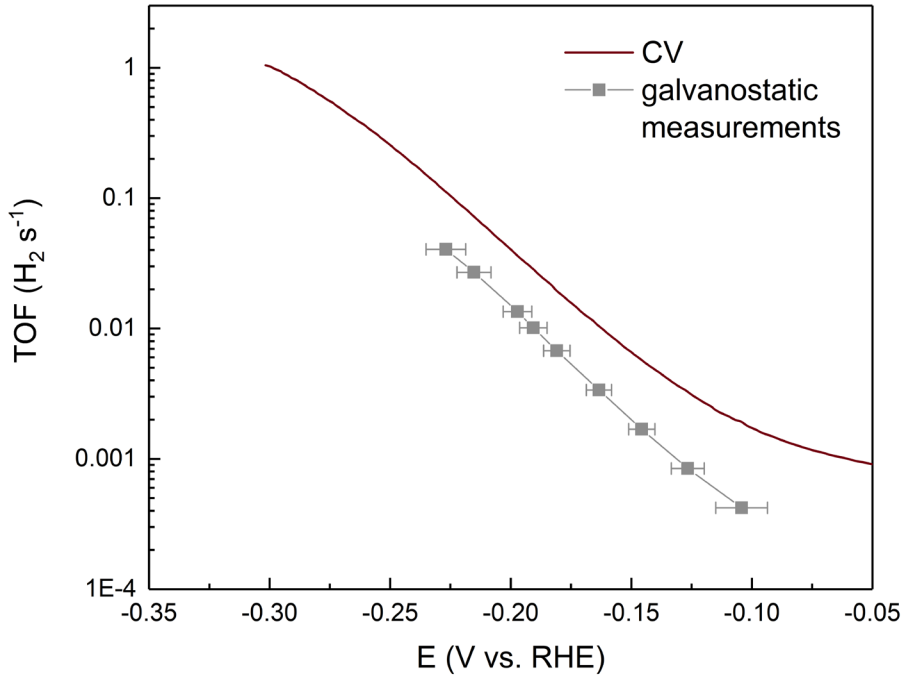

Figure S16. Turnover frequency (TOF) plot for Mo_2CT_x:Co (0.1 mg cm_{geo}^{-2} loading). CV measurements result in an overestimation of TOF values due to redox processes of the bulk material interfering with HER currents.

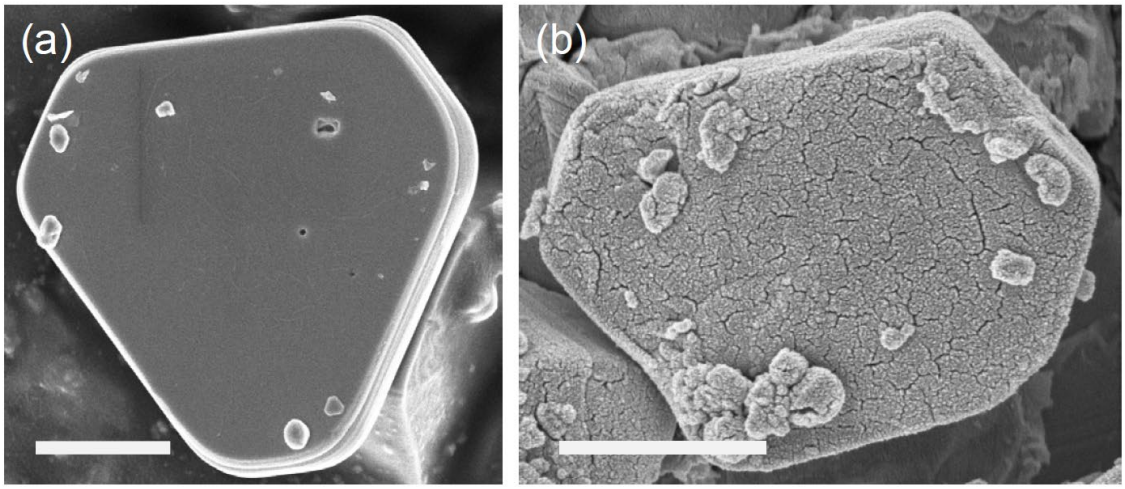

Figure S17. Comparison of the morphology of Mo_2CT_x:Co (a) before and (b) after HER catalysis by SEM imaging. Scale bar is 1μm.

References

(1) Deeva, E. B.; Kurlov, A.; Abdala, P. M.; Lebedev, D.; Kim, S. M.; Gordon, C. P.; Tsoukalou, A.; Fedorov, A.; Müller, C. R. In Situ XANES/XRD Study of the Structural Stability of Two-Dimensional Molybdenum Carbide Mo_2CT_x: Implications for the Catalytic Activity in the Water-Gas Shift Reaction. *Chem. Mater.* **2019**, *31*, 4505–4513.

(2) Le Bail, A. Whole Powder Pattern Decomposition Methods and Applications: A Retrospection. *Powder Diffr.* **2005**, *20*, 316–326.

(3) Rodríguez-Carvajal, J. Recent Advances in Magnetic Structure Determination by Neutron Powder Diffraction. *Phys. B Condens. Matter* **1993**, *192*, 55–69.

(4) Halim, J.; Kota, S.; Lukatskaya, M. R.; Naguib, M.; Zhao, M.-Q.; Moon, E. J.; Pitock, J.; Nanda, J.; May, S. J.; Gogotsi, Y.; et al. Synthesis and Characterization of 2D Molybdenum Carbide (MXene). *Adv. Funct. Mater.* **2016**, *26*, 3118–3127.

(5) Wei, C.; Rao, R. R.; Peng, J.; Huang, B.; Stephens, I. E. L.; Risch, M.; Xu, Z. J.; Shao-Horn, Y. Recommended Practices and Benchmark Activity for Hydrogen and Oxygen Electrocatalysis in Water Splitting and Fuel Cells. *Adv. Mater.* **2019**, *31*, 1806296.

(6) McCrory, C. C. L.; Jung, S.; Peters, J. C.; Jaramillo, T. F. Benchmarking Heterogeneous Electrocatalysts for the Oxygen Evolution Reaction. *J. Am. Chem. Soc.* **2013**, *135*, 16977–16987.

(7) Kresse, G.; Furthmüller, J. Efficient Iterative Schemes for Ab Initio Total-Energy Calculations Using a Plane-Wave Basis Set. *Phys. Rev. B* **1996**, *54*, 11169–11186.

(8) Kresse, G.; Furthmüller, J. Efficiency of Ab-Initio Total Energy Calculations for Metals and Semiconductors Using a Plane-Wave Basis Set. *Comput. Mater. Sci.* **1996**, *6*, 15–50.

(9) Kresse, G.; Joubert, D. From Ultrasoft Pseudopotentials to the Projector Augmented-Wave Method. *Phys. Rev. B* **1999**, *59*, 1758–1775.

(10) Perdew, J. P.; Burke, K.; Ernzerhof, M. Generalized Gradient Approximation Made Simple. *Phys. Rev. Lett.* **1996**, *77*, 3865–3868.

(11) Ling, C.; Shi, L.; Ouyang, Y.; Chen, Q.; Wang, J. Transition Metal-Promoted V_2CO_2 (MXenes): A New and Highly Active Catalyst for Hydrogen Evolution Reaction. *Adv. Sci.* **2016**, *3*, 1600180.